Isovector and isoscalar spin-multipole giant resonances in the parent and daughter nuclei of double-β-decay triplets

Elina Kauppinen ⊙* and Jouni Suhonen ⊙

Department of Physics, University of Jyväskylä, P.O. Box 35, FI-40014, Jyväskylä, Finland

The strength distributions, including giant resonances, of isovector and isoscalar spin-multipole transitions in the commonly studied double-β-decay triplets are computed in the framework of the quasiparticle random-phase approximation (QRPA) using the Bonn-A two-body interaction in no-core single-particle valence spaces. The studied nuclei include the double-β parent and daughter pairs (^{76}Ge, ^{76}Se), (^{82}Se, ^{82}Kr), (^{96}Zr, ^{96}Mo), (^{100}Mo, ^{100}Ru), (^{116}Cd, ^{116}Sn), (^{128}Te, ^{128}Xe), (^{130}Te, ^{130}Xe), and (^{136}Xe, ^{136}Ba). The studied transitions proceed from the ground states to the $J^\pi = 0^-$, 1^-, 2^- (spin-dipole transitions) and $J^\pi = 1^+$, 2^+, 3^+ (spin-quadrupole transitions) excited states in these nuclei. Comparison of the present results with potential future data may, indirectly, shed light on the reliability of QRPA-based nuclear-structure frameworks in description of the wave functions of nuclear states relevant for the two-neutrino and neutrinoless double β decays in the studied triplets.

I. INTRODUCTION

Two-neutrino double beta ($2\nu\beta\beta$) and neutrinoless double beta ($0\nu\beta\beta$) decays keep attracting keen attention of both the nuclear- and particle-physics communities. The $0\nu\beta\beta$ decay is of particular interest since, if detected, it has strong implications to physics beyond the standard model [1–7]. The $2\nu\beta\beta$ decay proceed through the 1^+ virtual states [1] and the $0\nu\beta\beta$ decay proceeds through virtual states of all multipolarities J^π [8,9] in the intermediate nuclei of the double-β-decay triplets consisting of an even-even mother, an odd-odd intermediate, and an even-even daughter nucleus. The wave functions of these virtual states can be probed by calculations and experiments on β^--type (from the 0^+ ground state of the $\beta\beta$ mother nucleus) and β^+-type (from the 0^+ ground state of the $\beta\beta$ daughter nucleus) isovector spin-multipole transitions to the $J^\pi = 0^-$, 1^-, 2^- ($L = 1$ spin-dipole transitions) and $J^\pi = 1^+$, 2^+, 3^+ ($L = 2$ spin-quadrupole transitions) excited states in the $\beta\beta$ intermediate nuclei. Here, L refers to the orbital angular momentum of the operator mediating the multipole transition. The corresponding theoretical studies have been conducted in [10] as an extension of the studies conducted in [11–13] for the 1^+ isovector spin-monopole resonances. Experimentally, these transitions have typically been probed by the partial-wave $L = 0$ charge-exchange reactions (CXRs) by using the β^- type of (p, n) or $(^3\text{He},t)$ reactions and β^+ type of (n, p), $(d,^2\text{He})$, or $(t,^3\text{He})$ reactions [6,14–16]. Recently, the partial-wave $L = 1$ CXRs to 2^- states have attracted interest by development of improved experimental methods and facilities, e.g., at the RCNP in Osaka, Japan [6,17].

In [10] the β^--type and β^+-type isovector spin-dipole (IVSD) and isovector spin-quadrupole (IVSQ) strength distributions and giant resonances in the $\beta\beta$-decay triplets ^{76}Ge–^{76}As–^{76}Se, ^{82}Se–^{82}Br–^{82}Kr, ^{96}Zr–^{96}Nb–^{96}Mo, ^{100}Mo–^{100}Tc$-^{100}$Ru, ^{116}Cd–^{116}In–^{116}Sn, ^{128}Te–^{128}I–^{100}Xe, ^{130}Te–^{130}I–^{130}Xe, and ^{136}Xe–^{136}Cs–^{136}Ba were studied using the proton-neutron quasiparticle random-phase approximation (*pn*QRPA). In the present work we extend these studies to non-CXR isoscalar and isovector spin-dipole (ISSD and IVSD) and isoscalar and isovector spin-quadrupole (ISSQ and IVSQ) strength distributions and giant resonances in the mother and daughter even-even nuclei of the listed $\beta\beta$-decay triplets. The corresponding transitions start from the 0^+ ground states and lead to the $J^\pi = 0^-$, 1^-, 2^- ($L = 1$ spin-dipole transitions), and $J^\pi = 1^+$, 2^+, 3^+ ($L = 2$ spin-quadrupole transitions) states in the same even-even nuclei. The $L = 1$ and $L = 2$ isovector transitions have been studied long ago by Auerbach and Klein for non-superfluid nuclei in the random-phase approximation (RPA) framework in [18]. For the description of spin-multipole transitions in superfluid nuclei, like in the present case, we have to use the charge-conserving quasiparticle RPA (QRPA) [19] instead of the above-mentioned charge-changing *pn*QRPA and charge-conserving RPA. Theoretical and experimental studies of the CXR and non-CXR type of transitions can probe indirectly the $\beta\beta$ decays by testing the ability of QRPA-based nuclear-theory frameworks (QRPA and *pn*QRPA) to yield reliable wave functions in both channels of transitions. In particular, in the *pn*QRPA and QRPA calculations the quantities to be probed are the single-particle valence spaces, the single-particle energies, and the resulting Bardeen-Cooper-Schrieffer (BCS) ground states as foundations of the correlated *pn*QRPA and QRPA ground states [19,20]. The relevant experiments include (p, p'), (e, e'), (α, α'), (d, d'), $(^3\text{He}, ^3\text{He}')$, etc., experiments [21].

---

*Corresponding author: elina.k.kauppinen@jyu.fi

II. THEORY

The formalism used in this work is the quasiparticle random phase approximation (QRPA). The formalism is explicitly introduced, for example, in [19]. Excitation energies of the observed nuclei are calculated as quasiparticle excitations of the QRPA ground state. The excitation operator in the QRPA case is

$$Q_\omega^\dagger = \sum_{a \leqslant b} \left[X_{ab}^\omega A_{ab}^\dagger(JM) - Y_{ab}^\omega \tilde{A}_{ab}(JM) \right], \quad (1)$$

where ω includes quantum numbers n, J^π, and M, and X_{ab}^ω and Y_{ab}^ω are the amplitudes that describe the probability of creating or annihilating a quasiparticle pair in the QRPA ground state. $A_{ab}^\dagger(JM)$ is the quasiparticle-pair creation operator

$$A_{ab}^\dagger(JM) = \mathcal{N}_{ab}(J)[a_a^\dagger a_b^\dagger]_{JM}, \quad (2)$$

and $\tilde{A}_{ab}(JM)$, the corresponding annihilation operator, is of the form

$$\tilde{A}_{ab}(JM) = (-1)^{J+M} A_{ab}(J-M)$$
$$= \mathcal{N}_{ab}(J)[\tilde{a}_a \tilde{a}_b]_{JM}. \quad (3)$$

Above the $\mathcal{N}_{ab}(J)$ is the normalization factor.

The QRPA equations can be written in a matrix form as

$$\begin{pmatrix} A & B \\ -B^* & -A^* \end{pmatrix} \begin{pmatrix} X^\omega \\ Y^\omega \end{pmatrix} = E_\omega \begin{pmatrix} X^\omega \\ Y^\omega \end{pmatrix}. \quad (4)$$

Matrices A and B are written explicitly in [19].

The transition operator for an isovector excitation can be written as

$$\mathcal{O}_{L,JM}^{0,\mathrm{v}} = i^L r^L [Y_L \sigma]_{JM} t_0, \quad (5)$$

and the isoscalar transition operator as

$$\mathcal{O}_{L,JM}^{0,\mathrm{s}} = i^L r^L [Y_L \sigma]_{JM}, \quad (6)$$

where t_0 is the third component of the isospin operator.

With the use of the transition operators (5) and (6) the reduced single-particle nuclear matrix elements (NMEs) can be calculated. For these operators the reduced single-particle NMEs can be written as

$$(a||\mathcal{O}_{L,J}^{0,\rho}||b) = (a||i^L r^L [Y_L \sigma]_{JM}||b)$$
$$= \sqrt{6} \hat{j}_a \hat{J} \hat{j}_b \frac{(-1)^{l_a}}{\sqrt{4\pi}} \hat{l}_a \hat{L} \hat{l}_b \begin{pmatrix} l_a & L & l_b \\ 0 & 0 & 0 \end{pmatrix}$$
$$\times \begin{Bmatrix} l_a & \frac{1}{2} & j_a \\ l_b & \frac{1}{2} & j_b \\ L & 1 & J \end{Bmatrix} \mathcal{R}_{ab}^{(L)} (-1)^{\frac{1}{2}(l_b-l_a+L)} \eta_{ab}^\rho, \quad (7)$$

where $\mathcal{R}_{ab}^{(L)}$ is a radial integral and ρ equals 's' or 'v' such that $\eta_{ab}^{\mathrm{s}} = 1$ and $\eta_{ab}^{\mathrm{v}} = 1$ if a and b denote neutron orbitals and $\eta_{ab}^{\mathrm{v}} = -1$ if a and b denote proton orbitals. Now the reduced transition NMEs can be written as

$$(nJ^\pi||\mathcal{O}_{L,J}^0||\mathrm{QRPA}) = -\sum_{a \leqslant b} \mathcal{N}_{ab}(J)(a||\mathcal{O}_{L,J}^0||b)$$
$$\times (v_a u_b - u_a v_b)(X_{ab}^{nJ^\pi} - Y_{ab}^{nJ^\pi}). \quad (8)$$

TABLE I. Pairing gap scaling parameters $g_{\mathrm{pair}}^{(\mathrm{n})}$ and $g_{\mathrm{pair}}^{(\mathrm{p})}$ for each nucleus are listed in columns 2 and 3. Also the particle-hole parameters for each J^π excitation are tabulated in columns 4–9.

Nucleus	$g_{\mathrm{pair}}^{(\mathrm{n})}$	$g_{\mathrm{pair}}^{(\mathrm{p})}$	g_{ph} for J^π					
			0^-	1^-	2^-	1^+	2^+	3^+
^{76}Ge	0.940	0.890	1.00	0.5732	0.975	1.000	0.5073	1.00
^{76}Se	0.975	0.910	1.00	0.5571	1.000	1.000	0.5042	1.00
^{82}Se	0.915	0.838	1.00	0.6511	1.000	1.000	0.5158	1.00
^{82}Kr	0.984	0.861	1.00	0.6516	1.000	1.000	0.5132	1.00
^{96}Zr	0.769	0.848	1.00	0.6464	1.000	1.000	0.5000	1.00
^{96}Mo	0.904	0.930	1.00	0.5829	1.000	1.000	0.5375	1.00
^{100}Mo	0.850	0.947	1.00	0.5438	1.000	1.000	0.4919	1.00
^{100}Ru	0.855	0.935	1.00	0.5440	1.000	1.000	0.4793	1.00
^{116}Cd	0.888	0.930	1.00	0.5757	1.000	1.000	0.5406	1.00
^{116}Sn	0.818	0.805	1.00	0.6159	1.000	1.000	0.4800	1.00
^{128}Te	0.860	0.810	1.00	0.6185	1.000	1.313	0.4682	1.00
^{128}Xe	0.863	0.877	1.00	0.5784	1.000	1.000	0.4664	1.00
^{130}Te	0.864	0.775	1.00	0.6122	0.860	1.000	0.4548	1.00
^{130}Xe	0.850	0.858	1.00	0.5888	1.000	1.257	0.4638	1.00
^{136}Xe	0.681	0.760	1.00	0.6510	1.000	1.000	0.4010	1.00
^{136}Ba	0.870	0.830	1.00	0.6001	1.000	1.394	0.4732	1.00

Transition strengths are calculated as the square of the transition NME

$$S_{nJ^\pi}^L = \left| (nJ^\pi||\mathcal{O}_{L,J}^0||\mathrm{QRPA}) \right|^2. \quad (9)$$

III. RESULTS AND DISCUSSION

The lowest quasiparticle energies for protons and neutrons are fitted to the proton and neutron pairing gaps. Pairing gaps for protons and neutrons are calculated by using the three-point formulas [19]

$$\Delta_p(A,Z) = \tfrac{1}{4}(-1)^{Z+1}[S_p(A+1,Z+1) - 2S_p(A,Z)$$
$$+ S_p(A-1,Z-1)],$$
$$\Delta_n(A,Z) = \tfrac{1}{4}(-1)^{A-Z+1}[S_n(A+1,Z) - 2S_n(A,Z)$$
$$+ S_n(A-1,Z)], \quad (10)$$

where S_p and S_n are the separation energies for protons and neutrons, respectively.

Also the lowest energies for each multipole are adjusted to the corresponding experimental ones by using the particle-hole parameter g_{ph}. The only exception are the 1^- states where the lowest one is spurious and has been removed from the calculations. Here, instead, the second 1^- state has been fitted to the lowest experimental 1^- energy. If the energy is not known experimentally (this is exclusively the case for the 0^- states) or the computed energy is not sensitive to the value g_{ph} (this is the case for most 1^+ and 3^+ states), the default value $g_A = 1.00$ is adopted. The resulting values of g_{ph} for each multipole state and each nucleus are also tabulated in Table I. The pnQRPA calculations are sensitive to the value of the particle-particle parameter g_{pp} [1,6,20], and its value can be fixed, e.g., by comparison with the measured half-life of a two-neutrino $\beta\beta$ transition, as was done in [10]. For QRPA the g_{pp} parameter plays a negligible role since the results are
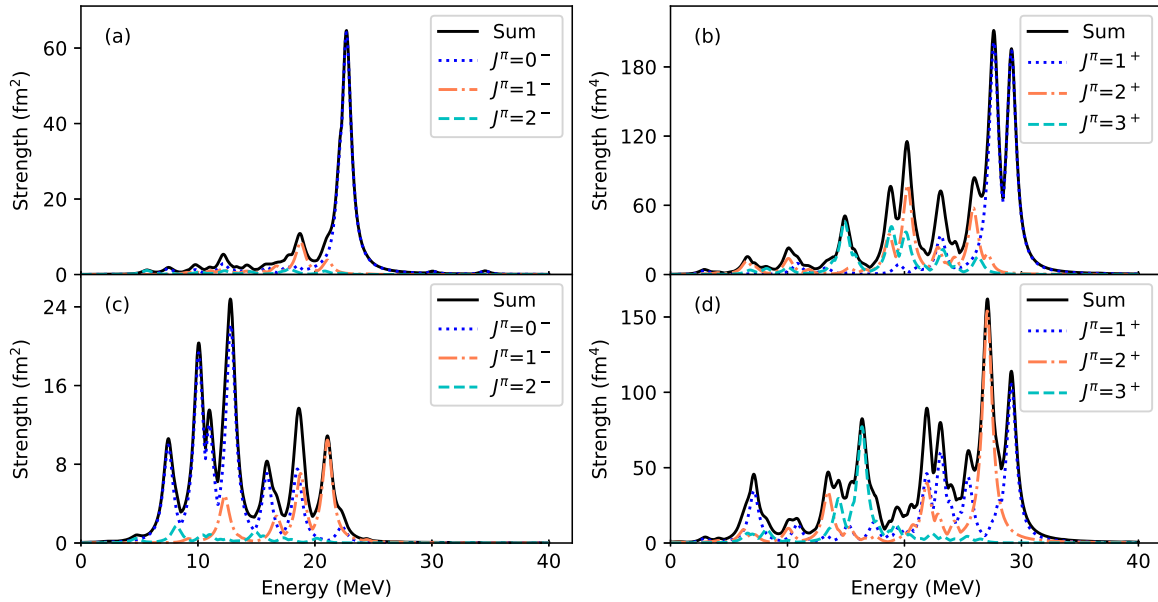
FIG. 1. Isovector and isoscalar multipole strength functions for ^{76}Ge. (a) isovector $L = 1$, (b) isovector $L = 2$, (c) isoscalar $L = 1$, and (d) isoscalar $L = 2$.

essentially independent of its value. This is why we adopted the default value $g_{pp} = 1.00$.

We calculate the strength (9) for each excitation energy E and multipolarity J^π. The corresponding discrete strength functions are then folded with a Lorentzian in order to make the strengths easier to compare with the potential future experimental data. For the Lorentzian we choose

$$F_L(E - E_0) = \frac{W}{\pi} \frac{1}{W^2 + (E - E_0)^2}, \tag{11}$$

as used also in [10]. In the Lorentzian fit (11) E is the excitation energy, E_0 is the energy of the peak, and W is the peak width which is set to 0.5 MeV following the convention of [10].

The computed strength functions are plotted as functions of E for a representative set of cases in Figs. 1–3, and the average energies and total strengths are given in Tables II and III. In Fig. 1, the strength functions are plotted for the ^{76}Ge nucleus for different transition types. Panel (a) in that figure presents the isovector strength for spin-dipole ($L = 1$) transitions, panel (b) presents the isovector strength for spin-quadrupole ($L = 2$) transitions, and panels (c) and (d) present the isoscalar strengths for the $L = 1$ and $L = 2$ transitions. In Fig. 2 the isoscalar strength functions for spin-quadrupole transitions for (a) ^{82}Se, (b) ^{82}Kr, (c) ^{96}Zr, and (d) ^{96}Mo nuclei are plotted. Finally, in Fig. 3 isovector and isoscalar strength functions for ^{136}Xe are shown the same way as in Fig. 1.

In spin-dipole transitions, the isovector strength is located almost only in one peak, as shown in Figs. 1 and 3. The dominant peak consists primarily of a 0^- state, and all other J^π states are almost negligible. This excitation is located at approximately 20 MeV for all the nuclei.

The isoscalar spin-dipole strengths are more spread than the isovector ones. In this case, the 0^- state is also the most

significant contributor to the strength function but also the 1^- state has a notable contribution. The largest strengths are observed in approximately around 10 MeV. From Figs. 1 and 3 and Tables II and III, it can be seen that the 2^- state has the lowest overall strength compared to the other multipoles, so it does not contribute to the total dipole strength functions very much.

Isovector spin-quadrupole strength functions are more spread in energy E than the spin-dipole ones. The strength function has its largest peak for a 1^+ state at about 30 MeV, as can be seen in Figs. 1 and 3. There is also a correlation between the mass number A and the ratio of the highest peak and other peaks: When A increases the largest peak gets more dominant. This correlation can also be seen in Figs. 1 and 2.

Lastly, the isoscalar spin-quadrupole strength is divided between all J^π states, which is different from the previously analyzed strength functions. The 2^+ and 1^+ states have the largest strength peaks, but the 3^+ state has a considerably large peak for some nuclei at approximately 15 MeV. These peaks are seen in Fig. 2. The strength is spread up to 30 MeV and is considerable at all energies. The total $L = 2$ strength is by far larger than the $L = 1$ strength, as seen in Tables II and III. For all nuclei the 1^+ strength is the largest and the 2^- spin-dipole strength the smallest. On average, the spin-quadrupole strength clearly increases with increasing mass number.

The presently obtained results for the isovector strength functions can also be compared with the corresponding strength functions for the charge-changing modes, calculated in Ref. [10]. In [10] the (p, n) β^--type and (n, p) β^+-type isovector strength functions were treated. For both the spin-dipole and spin-quadrupole transitions the strength distributions of the charge-changing modes are more widely spread. As discussed earlier, the isovector excitations in this work, as also in [10], tend to be concentrated in few

TABLE II. Average energies (columns 4 and 6) and total strengths (columns 5 and 7) for isovector (superscript v) and isoscalar (superscript s) spin-dipole and spin-quadrupole excitations for the nuclei with mass numbers $A = 76$, 82, 96, and 100. The average isovector energies $E_{\text{ave}}^{\text{v}}$ are compared with those of [10] (column 3), corrected for nuclear mass differences between the $\beta\beta$ intermediate nucleus and the $\beta\beta$ mother nucleus $[E(\text{GR})_-]$ or the $\beta\beta$ daughter nucleus $[E(\text{GR})_+]$. The energy $E(\text{GR})_-$ is listed for the $\beta\beta$ mother (β^- branch) and $E(\text{GR})_+$ for the $\beta\beta$ daughter (β^+ branch) in order to have the same initial nucleus for the charge-changing transitions of [10] and the charge-conserving ones of the present work. The strengths are given in units of fm^2 for $J^\pi = 0^-$, 1^-, 2^- and in fm^4 for $J^\pi = 1^+$, 2^+, 3^+.

| Nucleus	J^π	$E(\text{GR})_\pm$ (MeV)	$E_{\text{ave}}^{\text{v}}$ (MeV)	$S_{\text{tot}}^{\text{v}}$	$E_{\text{ave}}^{\text{s}}$ (MeV)	$S_{\text{tot}}^{\text{s}}$
^{76}Ge	0^-	19.163	21.533	193.84	12.403	144.43
	1^-	15.162	16.412	50.624	17.405	58.977
	2^-	17.050	14.728	20.446	12.602	21.384
	1^+	26.913	26.659	1038.9	22.727	979.92
	2^+	22.817	20.584	794.80	21.595	854.76
	3^+	19.696	18.596	503.73	16.758	523.29
^{76}Se	0^-	15.095	21.053	181.97	12.591	135.76
	1^-	10.343	16.343	48.181	17.303	55.843
	2^-	13.697	14.398	20.595	12.417	21.759
	1^+	23.671	27.157	1010.6	23.558	960.41
	2^+	19.927	21.183	751.68	22.232	804.63
	3^+	16.573	18.909	506.44	17.179	526.95
^{82}Se	0^-	16.923	21.238	216.42	12.411	162.07
	1^-	13.884	16.337	56.655	17.337	67.510
	2^-	15.382	14.807	23.031	12.542	24.357
	1^+	25.077	25.968	1083.8	22.183	1022.0
	2^+	22.785	19.939	902.78	20.779	975.70
	3^+	18.971	18.290	570.96	16.416	597.41
^{82}Kr	0^-	13.992	20.954	205.53	12.640	154.20
	1^-	10.801	17.353	54.409	18.279	64.385
	2^-	13.992	15.706	23.238	13.662	24.540
	1^+	23.146	26.432	1055.0	22.935	1001.5
	2^+	22.999	21.508	857.43	22.333	921.87
	3^+	21.622	20.864	575.54	19.059	600.43
^{96}Zr	0^-	31.028	20.106	266.58	11.179	199.60
	1^-	24.279	15.181	69.792	16.156	83.516
	2^-	22.045	13.851	27.743	11.623	29.502
	1^+	33.225	24.576	1800.2	20.217	1710.5
	2^+	26.539	18.888	1266.1	19.960	1366.0
	3^+	23.327	17.751	710.73	15.975	744.24
^{96}Mo	0^-	15.617	20.156	263.17	11.395	197.33
	1^-	11.513	15.116	69.461	15.989	81.699
	2^-	12.028	13.853	27.798	11.707	29.481
	1^+	23.662	25.142	1760.9	20.620	1662.3
	2^+	18.670	19.255	1256.6	20.397	1369.5
	3^+	14.506	17.773	731.13	15.995	765.79
^{100}Mo	0^-	25.300	19.826	268.76	11.193	199.57
	1^-	19.508	14.936	71.248	15.781	82.872
	2^-	18.148	13.570	29.344	11.512	31.185
	1^+	30.857	26.340	2856.1	21.315	2742.4
	2^+	23.888	20.037	1598.3	21.571	1715.5
	3^+	20.909	18.236	843.30	16.320	881.60
^{100}Ru	0^-	15.249	20.747	286.73	11.379	211.86
	1^-	11.073	15.478	73.597	16.370	85.756
	2^-	12.390	14.488	28.272	12.152	29.482
	1^+	24.655	27.238	2954.6	21.774	2808.5
	2^+	18.839	20.143	1649.1	21.629	1.75.9
	3^+	14.780	18.167	837.53	16.104	874.78
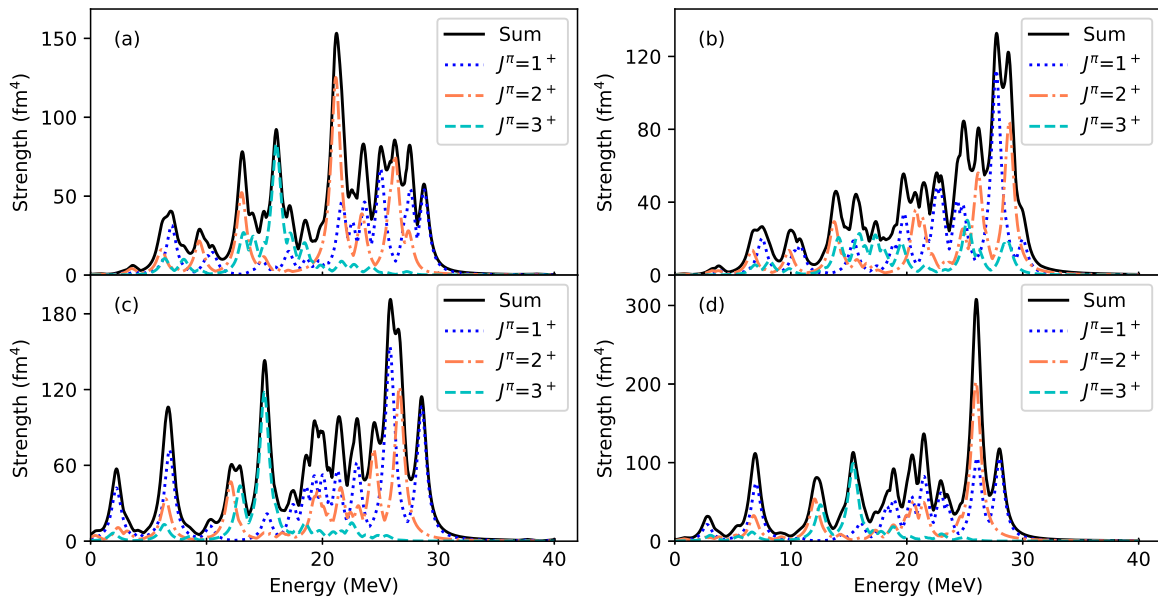
FIG. 2. Isoscalar $L = 2$ strength functions for four different nuclei. (a) ^{82}Se, (b) ^{82}Kr, (c) ^{96}Zr, and (d) ^{96}Mo.

peak-like structures rather than spreading over the whole excitation range, as in isoscalar excitations.

In Tables II and III the third column displays energies "$E(GR)_-$" and "$E(GR)_+$" from Table III of [10], corrected for mass differences between the $\beta\beta$ intermediate nucleus and the $\beta\beta$ mother and daughter nuclei, respectively. This is done because in [10] the average energies were referred to the ground state of the double-β intermediate nucleus, and in order to compare the general trends of average isovector energies with those of Ref. [18]. Since in [10] the feeding of the intermediate nuclei was discussed we have to adopt the "$E(GR)_-$" for the mother nuclei (^{76}Ge, ^{82}Se, ^{96}Zr, ^{100}Mo, ^{116}Cd, ^{128}Te, ^{130}Te, and ^{136}Xe) and "$E(GR)_+$" for daughter

nuclei (^{76}Se, ^{82}Kr, ^{96}Mo, ^{100}Ru, ^{116}Sn, ^{128}Xe, ^{130}Xe, and ^{136}Ba) of $\beta\beta$ decays. The average energies in Tables II and III reveal a common pattern, coincident with that found in [18]: The energies $E(GR)_-$, E^v_{ave}, and $E(GR)_+$ form on average a hierarchy, with $E(GR)_-$ being the largest, $E(GR)_+$ the smallest, and E^v_{ave} falling in the middle. This hierarchy is particularly distinct for the zirconium region of $A = 96$, as also was the case for ^{90}Zr in [18].

IV. CONCLUSIONS

The strength distributions of isovector and isoscalar spin-multipole transitions were studied in this work. The
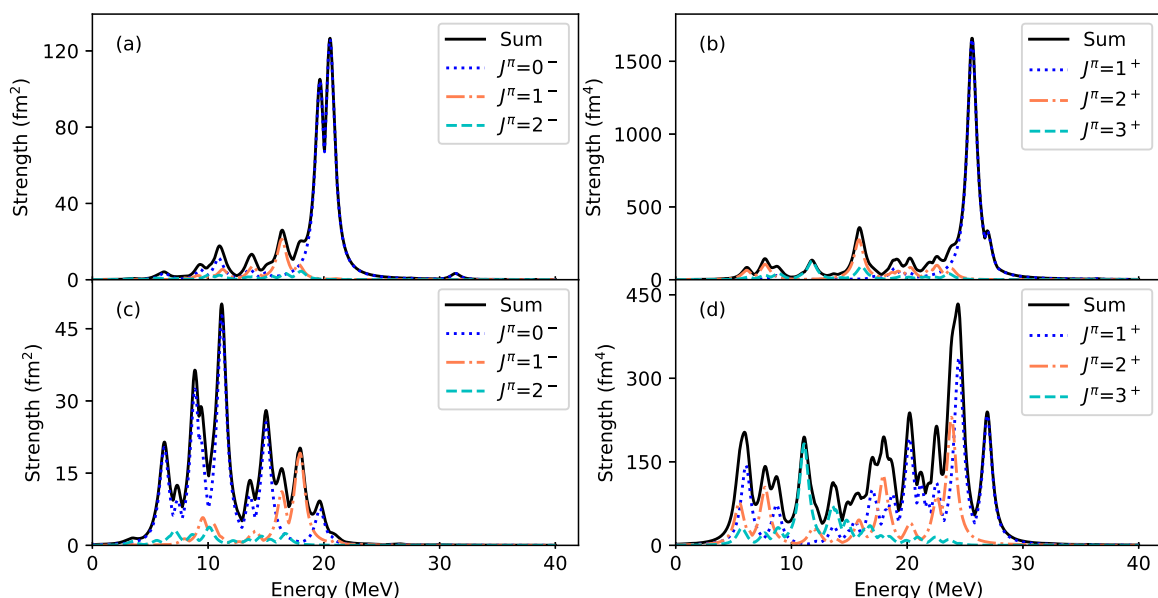

FIG. 3. Same as in Fig. 1 but for ^{136}Xe.

TABLE III. Same as in Table II but for the nuclei with mass numbers A = 116, 128, 130, and 136.

Nucleus	J^π	$E(GR)_\pm$ (MeV)	E_{ave}^v (MeV)	S_{tot}^v	E_{ave}^s (MeV)	S_{tot}^s
^{116}Cd	0^-	29.021	18.982	316.80	10.852	236.02
	1^-	22.732	14.306	83.147	15.011	97.805
	2^-	20.954	12.727	36.600	10.843	39.434
	1^+	34.166	26.423	3437.0	21.521	3308.2
	2^+	27.319	19.713	1989.0	21.175	2161.3
	3^+	24.279	17.391	1114.4	15.682	1170.2
^{116}Sn	0^-	15.324	18.970	326.10	10.632	241.92
	1^-	11.002	14.073	86.233	14.748	103.73
	2^-	13.065	12.590	37.224	10.613	40.582
	1^+	25.890	26.484	3605.1	21.393	3475.1
	2^+	20.040	19.164	2112.5	20.377	2291.8
	3^+	16.627	17.235	1146.6	15.457	1212.5
^{128}Te	0^-	23.632	19.626	397.56	10.926	299.35
	1^-	17.687	14.655	101.09	15.394	119.66
	2^-	17.813	13.639	40.022	11.432	42.042
	1^+	28.782	26.933	3774.8	20.510	3455.3
	2^+	23.372	18.280	2316.7	19.408	2502.7
	3^+	19.831	16.395	1273.2	14.777	1323.4
^{128}Xe	0^-	12.822	19.594	386.94	11.089	291.30
	1^-	9.474	14.739	98.806	15.485	115.50
	2^-	12.407	13.622	39.525	11.502	41.622
	1^+	23.963	25.558	3838.6	20.633	3655.0
	2^+	18.651	18.581	2288.5	19.748	2465.0
	3^+	15.572	16.651	1276.0	15.044	1328.9
^{130}Te	0^-	25.014	19.551	408.18	10.841	307.19
	1^-	19.248	14.489	104.16	15.184	123.20
	2^-	16.964	13.166	41.737	11.231	43.724
	1^+	27.702	25.494	3888.4	20.419	3685.5
	2^+	22.554	18.051	2372.5	19.110	2560.6
	3^+	19.158	16.173	1303.6	14.566	1354.4
^{130}Xe	0^-	15.069	19.601	399.73	11.056	301.10
	1^-	11.972	14.695	102.08	15.423	119.71
	2^-	12.824	13.637	40.557	11.470	42.702
	1^+	24.405	26.469	3826.6	20.389	3536.4
	2^+	19.513	18.305	2341.5	19.430	2524.5
	3^+	16.253	16.444	1308.2	14.851	1361.2
^{136}Xe	0^-	29.190	19.152	427.06	10.741	322.07
	1^-	23.466	14.316	108.75	14.971	129.96
	2^-	21.211	13.107	44.575	10.896	47.455
	1^+	28.289	24.708	3944.5	19.709	3740.9
	2^+	22.645	17.377	2461.8	18.157	2638.0
	3^+	19.814	15.579	1335.7	14.064	1394.5
^{136}Ba	0^-	12.917	19.253	419.82	10.927	316.70
	1^-	9.871	14.431	107.54	15.106	126.56
	2^-	12.205	13.293	43.740	11.127	46.544
	1^+	23.327	26.135	3843.7	19.551	3482.9
	2^+	18.766	17.717	2404.9	18.713	2600.4
	3^+	15.290	15.761	1338.6	14.258	1398.9

excitation energies and transition strengths were calculated using the QRPA formalism. The strength distributions were calculated for a set of double-β decaying nuclei and the corresponding daughter nuclei. The same double-β decaying nuclei were studied in [10] using the *pn*QRPA formal-ism for charge-changing isovector spin-multipole strength distributions.

In our QRPA calculations the quasiparticles were handled by using the BCS formalism, fitting the phenomenologi-cal proton and neutron pairing gaps with the help of the

corresponding pairing-strength parameters. Particle-hole parameters were adjusted so that the lowest proton and neutron quasiparticle energies were fitted to the proton and neutron pairing gaps. We also adjusted the energy of the lowest state for each multipole J^{π} to fit the data, if available. For this we used the particle-hole parameter, available in the QRPA formalism.

The isovector and isoscalar strength distributions for multipoles $L = 1$ and $L = 2$ were calculated. The average energies and total strengths were calculated and the distributions were plotted for representative cases and for each multipolarity containing the corresponding states $J^{\pi} = 0^{-}, 1^{-}, 2^{-}$ $(L = 1)$ and $J^{\pi} = 1^{+}, 2^{+}, 3^{+}$ $(L = 2)$.

The results show that the isoscalar strengths are more spread in energy than the isovector ones. The isovector spin-dipole strength is located almost only in one dominant peak, and for the spin-quadrupole strength, the most significant peak becomes more dominant when the mass number increases. The isoscalar transition-strength distributions show notable strength for all excitation states, contrary to isovector transitions.

Similarly to the previously made study [10], where the isovector multipole-strength distributions of β^{-} and β^{+} types of excitations were investigated, the presently studied isovector transition strengths tend to locate in one peak. Most of the nuclei had larger centroid energies in β^{-}-type excitations than those calculated in this study. The situation was the opposite for the β^{+}-type strength; the isovector excitation energies were lower on average than those calculated in this work.

When the experimental data are available, the results calculated in this work could be compared to the experimentally observed ones. Such comparison could shed light on the potency of a BCS-based random-phase-approximation framework to access high-lying excited states and their wave functions. Since the presently used QRPA and the charge-changing pnQRPA frameworks are based on the same quasiparticle mean field, the present study also serves as an indirect method to check the reliability of the pnQRPA framework in producing nuclear wave functions of high-lying states relevant for the studies of the nuclear matrix elements of the neutrinoless double β decay.

[1] J. Suhonen and O. Civitarese, Phys. Rep. **300**, 123 (1998).

[2] F. T. Avignone, S. R. Elliot, and J. Engel, Rev. Mod. Phys. **80**, 481 (2008).

[3] J. Maalampi and J. Suhonen, Adv. High Energy Phys. **2013**, 505874 (2013).

[4] J. T. Suhonen, Frontiers in Physics **5**, 55 (2017).

[5] J. Engel and J. Menéndez, Rep. Prog. Phys. **80**, 046301 (2017).

[6] H. Ejiri, J. Suhonen, and K. Zuber, Phys. Rep. **797**, 1 (2019).

[7] K. Blaum, S. Eliseev, F. A. Danevich, V. I. Tretyak, S. Kovalenko, M. I. Krivoruchenko, Y. N. Novikov, and J. Suhonen, Rev. Mod. Phys. **92**, 045007 (2020).

[8] J. Hyvärinen and J. Suhonen, Phys. Rev. C **91**, 024613 (2015).

[9] J. Hyvärinen and J. Suhonen, Adv. High Energy Phys. **2016**, 4714829 (2016).

[10] L. Jokiniemi and J. Suhonen, Phys. Rev. C **96**, 034308 (2017).

[11] I. Hamamoto and H. Sagawa, Phys. Rev. C **62**, 024319 (2000).

[12] D. R. Bes, O. Civitarese, and J. Suhonen, Phys. Rev. C **86**, 024314 (2012).

[13] O. Civitarese and J. Suhonen, Phys. Rev. C **89**, 044319 (2014).

[14] P. Puppe, D. Frekers, T. Adachi, H. Akimune, N. Aoi, B. Bilgier, H. Ejiri, H. Fujita, Y. Fujita, M. Fujiwara, E. Ganioğlu, M. N. Harakeh, K. Hatanaka, M. Holl, H. C. Kozer, J. Lee, A. Lennarz, H. Matsubara, K. Miki, S. E. A. Orrigo *et al.*, Phys. Rev. C **84**, 051305(R) (2011).

[15] J. H. Thies, D. Frekers, T. Adachi, M. Dozono, H. Ejiri, H. Fujita, Y. Fujita, M. Fujiwara, E.-W. Grewe, K. Hatanaka, P. Heinrichs, D. Ishikawa, N. T. Khai, A. Lennarz, H. Matsubara, H. Okamura, Y. Y. Oo, P. Puppe, T. Ruhe, K. Suda *et al.*, Phys. Rev. C **86**, 014304 (2012).

[16] D. Frekers, P. Puppe, J. H. Thies, and H. Ejiri, Nucl. Phys. A **916**, 219 (2013).

[17] D. Frekers, M. Alanssari, H. Ejiri, M. Holl, A. Poves, and J. Suhonen, Phys. Rev. C **95**, 034619 (2017).

[18] N. Auerbach and A. Klein, Phys. Rev. C **30**, 1032 (1984).

[19] J. Suhonen, *From Nucleons to Nucleus: Concepts of Microscopic Nuclear Theory* (Springer, Berlin, 2007).

[20] J. Suhonen, T. Taigel, and A. Faessler, Nucl. Phys. A **486**, 91 (1988).

[21] J. Speth and A. van der Woude, Rep. Prog. Phys. **44**, 719 (1981).